

Discrete Cosine Transform-Driven Hybrid Orthogonal Polynomials: Design and Applications in Signal Processing

Mariam Taha Yassen
Sadiq H. Abdulhussain

Department of Computer Engineering
University of Baghdad
10071 Al-Jadriya,, Baghdad, Iraq
gs22.mtyaseen@coeng.uobaghdad.edu.iq; sadiqhabeeb@coeng.uobaghdad.edu.iq

Received January 23, 2025, revised March 17, 2025, accepted March 17, 2025.

ABSTRACT. *In the field of digital image and speech signal processing, orthogonal polynomials play a significant role in characterizing, processing, and analyzing signals due to their unique properties. This paper introduces three new hybrid forms of orthogonal polynomials: Discrete Cosine Krawtchouk Tchebichef transform (DCKTT), Discrete Cosine Krawtchouk Tchebichef Krawtchouk transform (DCKTKT), and Discrete Krawtchouk Tchebichef Krawtchouk Cosine transform (DKTKCT). These forms combine Discrete Cosine Transform (DCT), Discrete Krawtchouk Polynomials (KrP), and Discrete Tchebichef Polynomials (TcP) to enhance signal processing capabilities. We provide the mathematical and theoretical frameworks for these hybrid forms and conduct a comparative study using a well-known database to evaluate their performance. The evaluation focuses on key properties such as energy compaction, localization, and feature extraction. Experimental results demonstrate that DCKTT achieves superior energy compaction, while DCKTKT and DKTKCT excel in localization. Additionally, we apply the proposed forms to steganography and numerical recognition, showing significant improvements in embedding capacity and feature extraction accuracy. This work advances the state-of-the-art in signal processing and opens new avenues for applications in image compression, speech recognition, and secure data embedding.*

Keywords: Discrete Cosine Transform, Discrete orthogonal polynomial, hybrid form, steganography, numerical recognition.

1. **Introduction.** The innovative technologies in the different fields of recent life, such as the Internet of Things (IoT), digital signal processing, information analysis and security. These have led to an increase demand for extracting valuable information or enhance the quality of the signal (audio, image and video). For example, Images become digital and enter into many fields prompting researchers to make great efforts in the field of image signal processing by focusing on considerable areas such as analysis and enhancement of visual information for human interpretation and processing of image data for tasks such as storage, transmission, and extraction of visual features. Moreover, speech signal processing emerged and received the attention of many researchers in terms of speech analysis, noise removal, and ensuring the accuracy of the recording and reception of speech signals. Various methods have been used to analyze, process and interpret signals such as: filtering [1], spectral analysis [2], time-frequency analysis [3], machine learning and deep learning [4].

Discrete Transforms are considered one of the methods for signal processing and analysis. They play an essential role in facilitating the processing of signals by presenting them in different representations and domains to perform specific operations more efficiently. There are different types of discrete transforms depend on numerous types of orthogonal polynomials such as Tchebichef polynomial (TcP) [5], Krawtchouk polynomial (KrP) [6, 7], Charlier polynomial (ChP) [8], wavelet polynomial (WaP) [9] and Hahn polynomial (HaP) [10].

The performance of each polynomial depends mainly on its characteristics that make it distinct from others and enable it to be used in specific applications. Basically, the robustness of any type of discrete transform is characterized by different properties like data compression, localization, numerical stability, strength against noise, effective data processing, and feature extraction [11].

Energy compaction (EC) is considered one of the most significant property of the transformation method. It concentrates the signal's energy in a smaller subset of transformation coefficients [12] and can be measured through the calculation of the proportion of the number of coefficients that contains most of the signal energy to the total number of coefficients. Energy compaction is the key principle behind data compression that needs to be stored or transmitted without significant loss of information. DCT is an example of a transform with a good energy compaction as it has a high energy compaction that makes it more significant in video and audio compression applications [12].

Whilst DCT lacks localization in space which means that the basis functions of DCT do not provide information about where a particular frequency is present in the signal [11]. In other words, its basis functions depict the spatial frequency resolution and lacks the ability to represent the time event. In such cases, localization is a fundamental property of a transformation. Localization reveals a close relationship between the transformed signal and the original signal's structure. This means that the localization property implies detailed information within the region of interest (ROI) of the desired features within a signal. In other words, the location of the ROI in the original and transformed domains [11].

Orthogonal moments are generated using orthogonal polynomials and they are widely used in the field of speech and image applications, such as data compression [13–16], speech enhancement [17], face recognition [18], pattern recognition [19], watermarking and encryption [20–23], edge detection [24], and classification and detection [25–27]. They provide a good performance in different fields. To increase the efficacy of these functions by enhancing the different properties such as localization in space and to provide robust feature extraction, a new set of orthogonal functions has been presented by different researchers as in [17, 28, 29].

These functions are presented based on the idea of fusing multiple orthogonal polynomials to develop a new hybrid forms which widely used in recent and various fields of signal processing. Both Discrete Tchebichef Transform (DTcT) and Discrete Krawtchouk Transform (DKrT) are deemed as the most significant discrete orthogonal polynomials that are used in the hybrid forms combinations and have different characteristics in term of Energy Compaction and Localizations Property. DTcT has superior energy compaction compared to DCT [5]. This is the main reason why it is used in the compression of video and audio [30]. On the other hand, DKrT has high localization property [6]; therefore, it is known for its ability in extracting features from signals effectively.

Motivated by the idea of fusing multiple orthogonal polynomials (OPs) provides higher performance and based on the concept that the combination of multiple OPs also generates an orthogonal polynomial [31], this paper proposed a new sets of functions using a powerful set of orthogonal functions with enhanced capabilities. As far as we know, no previous

study has utilized DCT in the combination with other OPs. Therefore, in this work, we concentrate on establishing the new OPs by combining DCT with other powerful transforms since they already approved advantageous properties. The main contributions of the proposed work are listed as follows:

- A mathematical formulas have been conducted to investigate the use of DCT transformation as an intrinsic parameter in the different hybrid OP.
- A mathematical analysis of the proposed hybrid OPs is performed to examine the localization and energy compaction properties.
- A comparison between the proposed hybrid forms and the recent hybrid form of OP called SKTP in terms of the significant properties is implemented.
- The capability of the proposed OPs is evaluated by utilizing them in two applications: numerical recognition and steganography.

The structure of this paper is as follows: In Section 2, the mathematical forms of OPs (TcP, KrP and DCT) with the orthogonal moments' computation is provided. In Section 3, the proposed OPs are presented. In Section 4, the performance evaluation of the proposed OPs and a comparison to existing hybrid OPs are introduced. In Section 5, numerical recognition and steganography applications are used to assess the proposed polynomials. Finally, Section 6 presents the conclusion of this paper.

2. Fundamental Concepts of Orthogonal Polynomials (OPs) and Moments.

This section provides the mathematical foundations and fundamental concepts of the OPs utilized in this paper. It includes the preliminaries of discrete orthogonal polynomials and the definitions of orthogonal moments.

2.1. Tchebichef Polynomials. The definition of the classical and scaled Tchebichef polynomial (TcP) of n th order is determined by [32]:

$$T_n(x) = \sqrt{\frac{\omega_T(x)}{\rho_T(n)}} (1-N)_n {}_3F_2(-n, -x, 1+n; 1, 1-N; 1), \quad (1)$$

$$n, x = 0, 1, \dots, N-1,$$

where $\omega_T(x)$ is the weight function and $\rho_T(n)$ is the squared norm of the TcP. Mathematically, they are expressed as follows [33]:

$$\omega_T(x) = 1, \quad (2)$$

$$\rho_T(n) = (2n)! \binom{N+n}{2n+1}, \quad (3)$$

therefore, 1 can be rewritten as follows:

$$T_n(x) = (1-N)_n {}_3F_2(-n, -x, 1+n; 1, 1-N; 1) \frac{1}{\sqrt{(2n)! \binom{N+n}{2n+1}}}, \quad (4)$$

where $\binom{a}{b}$ is the binomial coefficients and equal to $\frac{a!}{b!(a-b)!}$, ${}_3F_2$ is the hypergeometric function determined by [34]:

$${}_3F_2(-n, -x, 1+n; 1, 1-N; 1) = \sum_{k=0}^{\infty} \frac{(-n)_k (-x)_k (1+n)_k}{(1)_k (1-N)_k k!}, \quad (5)$$

where $(a)_k$ is the Pochhammer symbol and it is defined by [32, 35]:

$$(a)_k = \frac{\Gamma(a+k)}{\Gamma(a)} = a(a+1)(a+2) \cdots (a+k+1). \quad (6)$$

The computation of the TcP coefficients by utilizing the hypergeometric and gamma functions suffers from numerical instability. In addition, these functions results in high execution time. Thus, the three-term recurrence (TTR) relation is applied when computing the Tchebichef polynomial coefficients [36–38]. Mukundan *et al.* [32] introduce the recurrence relation of n -direction TcP coefficients as follows:

$$T_n(x) = \beta_1 T_{n-1}(x) + \beta_2 T_{n-2}(x) \quad (7)$$

$$\beta_1 = (2x + 1 - N)/n\sqrt{(4n^2 - 1)/(N^2 - n^2)}, \quad (8)$$

$$\beta_2 = (1 - n)/n\sqrt{(2n + 1)/(2n - 3)}\sqrt{(N^2 - (n - 1)^2)/(N^2 - n^2)}, \quad (9)$$

$$n = 2, 3, \dots, N - 1, \quad x = 0, 1, \dots, N - 1,$$

with initial conditions:

$$T_0(x) = \frac{1}{\sqrt{N}}, \quad (10)$$

$$T_1(x) = (2x + 1 - N)\sqrt{\frac{3}{(N(N^2 - 1))}}. \quad (11)$$

This recurrence relation falls short for signals of larger sizes than 81 samples. To tackle this challenge, the recurrence relation in the x -direction is utilized [39]:

$$T_n(x) = \alpha_1 T_n(x - 1) + \alpha_2 T_n(x - 2), \quad (12)$$

$$\alpha_1 = \frac{-(2x - 1)(x - N - 1) - x - n(n + 1)}{(N - x)x}, \quad (13)$$

$$\alpha_2 = \frac{(x - N - 1)(x - 1)}{(N - x)x}, \quad (14)$$

$$n = 1, 2, \dots, N - 1; \quad x = 2, 3, \dots, N/2 - 1$$

and the initial values [40]:

$$T_n(0) = -\sqrt{\frac{(N - n)}{(N + n)}}\sqrt{\frac{(2n + 1)}{(2n - 1)}}T_{n-1}(0), \quad (15)$$

$$n = 1, 2, \dots, N - 1$$

$$T_n(1) = \left(1 + \frac{(n(1 + n))}{(1 - N)}\right) T_n(0), \quad (16)$$

$$n = 0, 1, \dots, N - 1$$

$$T_0(0) = \frac{1}{\sqrt{N}} \quad (17)$$

It is noteworthy that the recurrence relation in Eq. 12 is applied up to $x = N/2 - 1$. Therefore, the TcP coefficients are computed using the symmetry relation:

$$T_n(N - 1 - x) = (-1)^n T_n(x), \quad (18)$$

$$n = 0, 1, \dots, N - 1, \quad x = N/2, N/2 + 1, \dots, N - 1$$

In this paper, the three-term recurrence relation TTR presented in [5] is utilized to compute the Tchebichef polynomial as this TTR handles signals with a large size than 6144 samples with less computational complexity.

2.2. Krawtchouk Polynomials. The definition of Krawtchouk polynomial (KrP) of n th order, $K_n(x; p)$ is given by [7]:

$$K_n(x; p, N - 1) = \sqrt{\frac{\omega_K(x)}{\rho_K}} {}_2F_1\left(-n, -x; -N + 1; \frac{1}{p}\right), \tag{19}$$

$$p \in (0, 1)$$

where $\omega_K(x)$ and $\rho_K(x)$ are the weight squared norm functions of the KrP. The definitions of these functions are [41]:

$$\omega_K(x) = p^x \binom{N - 1}{x} (1 - p)^{N - x - 1} \tag{20}$$

$$\rho_K(n) = (-1)^n \frac{n!}{(-N + 1)_n} \left(\frac{1 - p}{p}\right)^n \tag{21}$$

${}_2F_1$ represents the hypergeometric function of KrP and it is defined by [42]:

$${}_2F_1\left(-n, -x; -N + 1; \frac{1}{p}\right) = \sum_{k=0}^{\infty} \frac{(-n)_k (-x)_k}{(-N + 1)_k k!} \left(\frac{1}{p}\right)^k \tag{22}$$

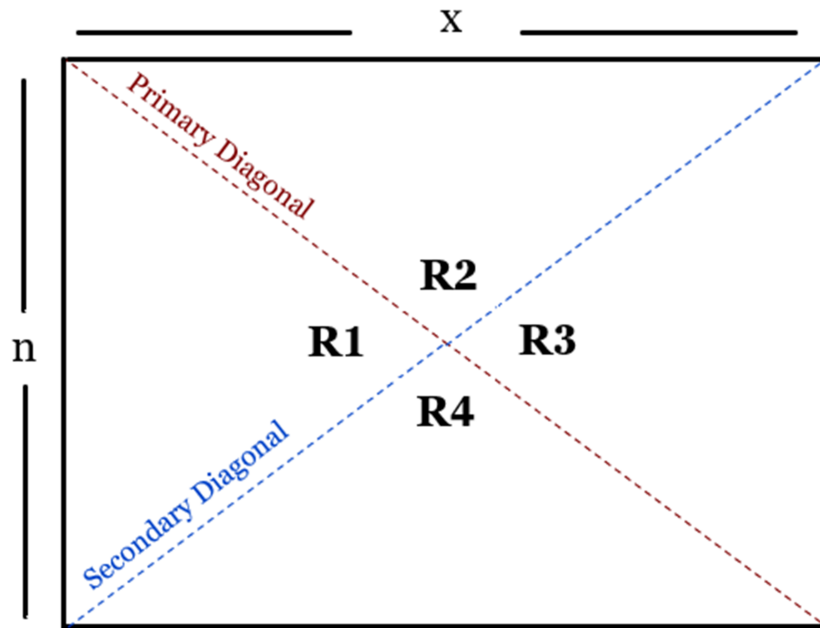


FIGURE 1. The four parts of the KrP plane [7].

By adjusting the values of the control parameter (p), the KrP demonstrated its ability to extract features from different ROIs in the image [43]. Because of utilizing the hypergeometric and gamma functions in the KrP coefficients computations, the TTR relation is employed. Several studies have focused on implementing TTR relation in [38, 43, 44]. In this paper, the TTR algorithm presented in [7] is used. The n -direction recurrence relation is used in bi-directional form (forward and backward). This algorithm partitioned the KrP plane along with the primary and secondary diagonals into four triangular parts (R1, R2, R3, and R4), as shown in Figure 1. KrP coefficients are directly computed for one part, while the other parts are determined by employing the symmetry relations. This algorithm has demonstrated an improvement for a wide range of the control parameter p in terms of coefficients accuracy, and computation complexity. In addition, it is capable

of handling large sized signals. To compute the KrP coefficients, the following steps are employed [7]:

1. First, $K_n(0)$ and $K_n(1)$ are obtained:

$$K_0(0) = \sqrt{(1-p)^{(N-1)}}, \quad (23)$$

$$K_n(0) = \sqrt{\frac{p(N-n)}{(1-p)n}} K_{n-1}(0), \quad (24)$$

$$n = 1, 2, \dots, N-1$$

$$K_n(1) = \frac{-n + (N-1)p}{(N-1)p} \sqrt{\frac{(N-1)p}{(1-p)}} K_n(0), \quad (25)$$

$$n = 0, 1, \dots, N-2$$

2. The TTR in the n -direction is used to compute the KrP coefficients in part R1 as follows:

$$\gamma_1 K_n(x+1) = \gamma_2 K_n(x) + \gamma_3 K_n(x-1), \quad (26)$$

$$\gamma_1 = \sqrt{p(1-p)(N-x-1)(x-1)}, \quad (27)$$

$$\gamma_2 = -n + p(N-x-1) + (1-p)x, \quad (28)$$

$$\gamma_3 = \sqrt{p(1-p)x(N-x)} \quad (29)$$

3. The coefficients of R2 is obtained using the symmetry relation about the primary diagonal ($n = x$):

$$K_n(x) = K_x(n) \quad (30)$$

4. The coefficients of parts R3 and R4 are computed by employing the symmetry relation of the secondary diagonal ($(n = N - x - 1)$)

$$K_{N-x-1}(x) = (-1)^{N-n-x-1} K_n(x) \quad (31)$$

5. For large signal size and to avoid zero initial values, the KrP coefficients for control parameter $p > 0.5$ are computed using the relation [7]:

$$K_n(x; 1-p) = (-1)^n K_n(N-x-1; p) \quad (32)$$

2.3. Discrete cosine transform (DCT). The DCT basis functions is calculated by the following Eq. given by [12, 28, 45]:

$$\alpha_n(x) = \begin{cases} \sqrt{\frac{1}{N}} & \text{for } n = 0 \\ \sqrt{\frac{1}{N}} \cos\left(\frac{\pi n}{2N}(2x+1)\right) & \text{for } n > 0 \end{cases} \quad (33)$$

The DCT has distinct properties such as it is a real function of real values of -1 to 1 [12], fast transform and does not require complex mathematics [12], and has excellent energy compaction for images [12, 46–48].

2.4. Orthogonal Moments. Orthogonal moments are defined as scalar quantities obtained from projections of signal onto orthogonal basis functions. These functions are considered superior in facilitating efficient processing and analysis as well as minimizing redundancy [3]. Thus, it is employed for approximating solutions for differential equations [49]. For the one dimension signal $f(x)$ with a length of N samples, the moment Φ_n

is computed by the following formula [50]:

$$\Phi_n = \sum_{x=0}^{N-1} R_n(x; N) f(x), \quad (34)$$

$$n = 0, 1, \dots, N - 1$$

where $R_n(x; N)$ represents the OP. To reconstruct the signal $f(x)$, the following equation is used:

$$\hat{f}(x) = \sum_{n=0}^{N-1} R_n(x; N) \Phi_n, \quad (35)$$

$$x = 0, 1, \dots, N - 1$$

On the other hand, for the two dimension signal of size $N \times N$, the moments are computed as follows [50]:

$$\Phi_{nm} = \sum_{y=0}^{N-1} \sum_{x=0}^{N-1} R_n(x; N) R_m(y; N) f(x, y), \quad (36)$$

$$n, m = 0, 1, \dots, N - 1$$

The 2D signal is reconstructed is carried out using the following formula:

$$\hat{f}(x, y) = \sum_{n=0}^{N-1} \sum_{m=0}^{N-1} R_n(x; N) R_m(y; N) \Phi_{nm}, \quad (37)$$

$$x = 0, 1, \dots, N - 1$$

$$y = 0, 1, \dots, N - 1$$

3. The Proposed Discrete Hybrid Forms of Orthogonal Polynomials. In general, to facilitate signal handling and efficient analysis of signal components, orthogonal polynomials are used. The signal can be expressed in the moments domain with less number of moments that characterize its information, which improves the features extraction and the processing of the signal [51]. Mathematically, the combination (multiplication) of different OP orthogonal polynomials results in a new OP [52]. By conducting various tests and attempts to obtain new hybrid functions that meet the best improved localization and energy compaction properties compared to current hybrid forms. This section presents three different types of proposed OP, namely Discrete Cosine-Krawtchouk-Tchebichef transform (DCKTT), Discrete Cosine-Krawtchouk-Tchebichef-Krawtchouk transform (DCKTKT), and Discrete Krawtchouk-Tchebichef-Krawtchouk-Cosine Transform (DKTKCT). The proposed polynomial is derived from multiplying well-known effective functions to get the desired properties. These polynomials are defined in the following sections.

3.1. Discrete Cosine-Krawtchouk-Tchebichef Transform (DCKTT). This hybrid form is acquired from the first level combination of a well-known OP and formed from a Cosine transform multiplied by Krawtchouk [43] and Tchebichef [32] polynomials. The formula of the hybrid form of the n th order $R_n(x)$ is implemented based on the following mathematical equation:

$$R_n(x; N) = \sum_{j=0}^{N-1} \alpha_j(N) K_j(x; N) T_j(n; N), \quad (38)$$

$$n, x = 0, 1, \dots, N - 1$$

where $K_j(x; N)$, $T_j(n; N)$, and $\alpha_j(N)$ are the mathematical formula of KrP, TcP, and DCT polynomials respectively.

The matrix form of the DCKTT is written as follows:

$$R = Q_C^T Q_K Q_T = R_{DCKT} \quad (39)$$

where Q_K , Q_C and Q_T are the matrix forms of $X_n(x; N)$, $Z_n(x)$, and $Y_n(x; N)$ polynomials, respectively. Note that (Qc)T represents the matrix transpose for DCT. To clarify the moment distribution of the proposed OP, Figure2 shows a 3D plot of the DCKTT of Cameraman test image of size 128×128 using control parameters $p = 0.5$, and $N = 128$. It can be noted that the high energy moments of DCKTT, which carries the signal information are distributed in the range $x, n = 0, \dots, N/4$, where the highest distribution of most moments is concentrated in that region. While signal details (low energy moments) are distributed from the first quarter toward $N - 1$ for x and n directions; therefore, this hybrid form has a high level of energy compaction property compared to the original OP forms.

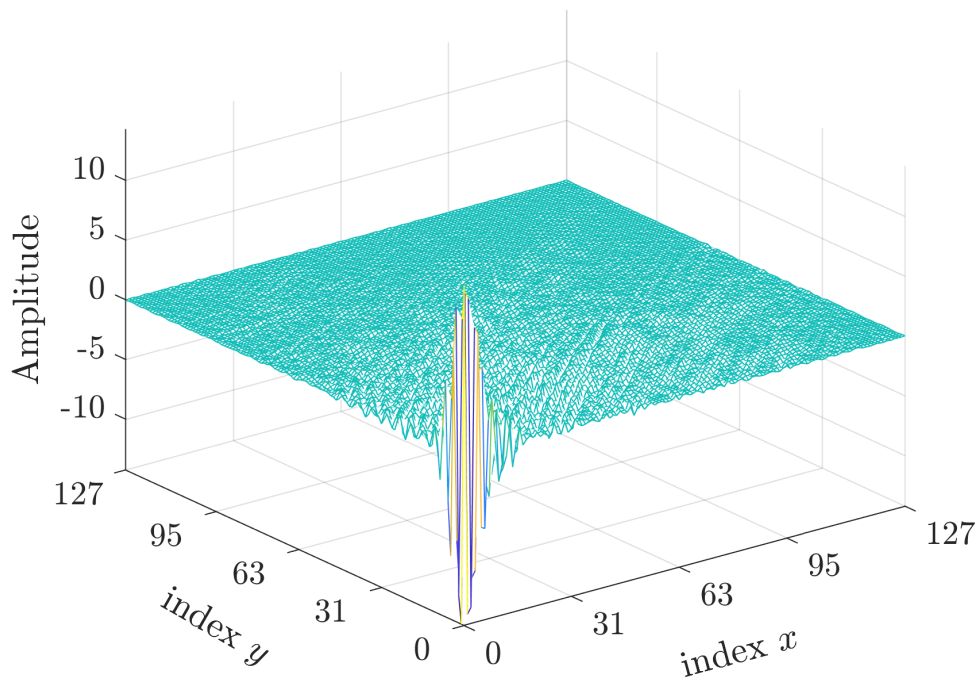


FIGURE 2. The 3D plot of moment distribution of the proposed polynomial in the DCKTT domain.

3.2. Discrete Cosine-Krawtchouk-Tchebichef-Krawtchouk Transform (DCKTKT). KrP is considered stellar in terms of extracting local features from any region-of-interest in the signals [7]. Accordingly, this provides a clear relationship between the transform coefficients and time function, which improves the polynomial ability of feature extraction. Therefore, by embedding KrP to the proposed DCKTT, the localization property will be enhanced. The hybrid form mathematical equation of the n th order of DCKTKT, $R_n(x)$, is given by:

$$R_n(x; N) = \sum_{j=0}^{N-1} \alpha_j(N) T_j(x; N) K_j(n; N), \quad (40)$$

$$n, x = 0, 1, \dots, N - 1$$

where $K_j(x; N)$, $T_j(n; N)$, and $\alpha_j(N)$ are KrP, TcP and DCT, respectively. The matrix representation of the DCKTKT can be depicted as follows:

$$R = Q_C^T Q_K Q_T^T Q_K = R_{DCKTK} \tag{41}$$

Where Q_K , Q_C and Q_T are the matrix form of the $X_n(x; N)$, $Z_n(x)$, and $Y_n(x; N)$ polynomials, respectively. Note that Q_C^T , Q_T^T represents the matrix transpose for DCT and DTHT, respectively. To clarify the moment distribution of this OP, Figure 3 shows the 3D plot of the DCKTKT of Cameraman test image of size 128×128 using the control parameters of $p = 0.5$ and $N = 128$. It is noticed that the moments distribution of the polynomial are symmetrical and the high order coefficients are distributed across the four corners. The range of $n = 0, 1, \dots, N/2 - 1$ belongs to the right part of the image, while the moments in the range $n = N/2, N/2 + 1, \dots, N - 1$ are linked with the left part of the image. Thus, moment indicators in the moment domain are related to signal indicators in the signal domain which provide a good analysis of the desired signal.

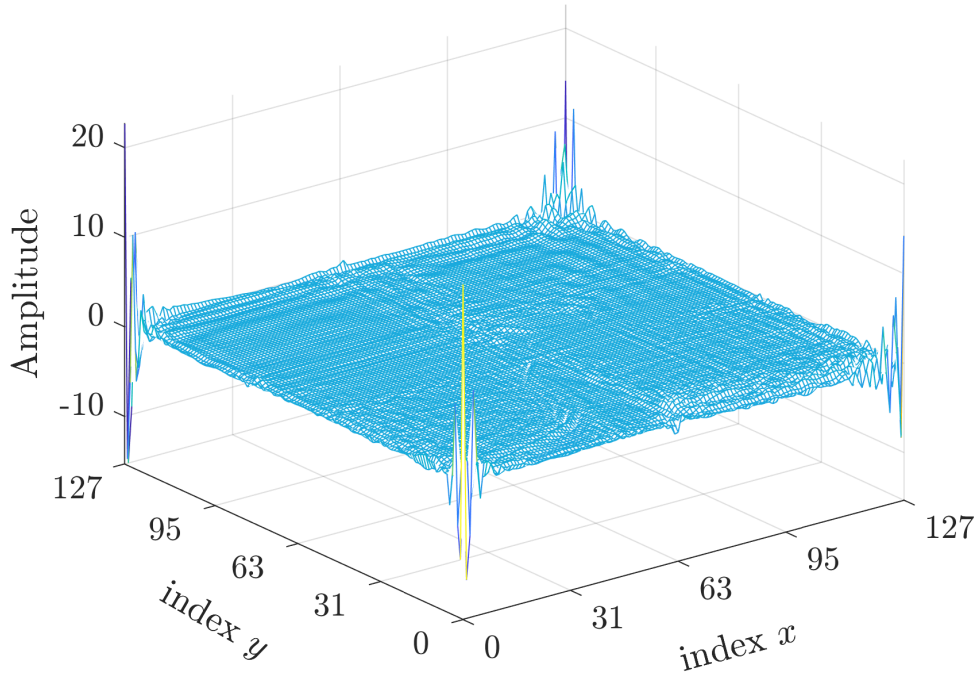


FIGURE 3. The 3D plot of moment distribution of the proposed polynomial in the DCKTKT domain.

3.3. Discrete Krawtchouk-Tchebichef-Krawtchouk-Cosine Transform (DKTKCT).

Through implementing various tests and attempts to obtain new hybrid functions that meet the best improved localization and energy compaction properties compared to current hybrid forms, the new hybrid form of OP termed as DKTKCT is introduced. The n th order of DKTKCT, $R_n(x)$, is formed as follows:

$$R_n(x; N) = \sum_{j=0}^{N-1} K_j(x; N) T_j(n; N) K_j(x; N) \alpha_j(N), \tag{42}$$

$$n, x = 0, 1, \dots, N - 1$$

where $K_j(x; N)$, $T_j(n; N)$ and $\alpha_j(N)$ are orthogonal polynomials resulted from KrP, TcP and DCT, respectively. It is important to note that the order in which mathematical equations of the OP are multiplied has the greatest influence in determining the

properties of the resulted OP. Therefore, in this research, many attempts were made to obtain the most appropriate order that gives the required better properties. The matrix representation of the DKTKCT can be depicted as follows:

$$R = Q_K Q_T Q_K Q_C = R_{DKTKC} \quad (43)$$

where Q_K , Q_C and Q_T are the matrix form of the $X_n(x; N)$, $Z_n(x)$, and $Y_n(x; N)$ polynomials, respectively. Figure 4 shows the 3D plot of the DKTKCT for an image of size 128×128 using the control parameters of $p = 0.5$ and $N = 128$. It can be noticed that the moments with high energy are distributed in the middle which hold the signal information. On the other hand, the moments energy is reduced when moving to corners where the details of the signal are located. From these specified properties, we can select the appropriate OP based on the type of applications.

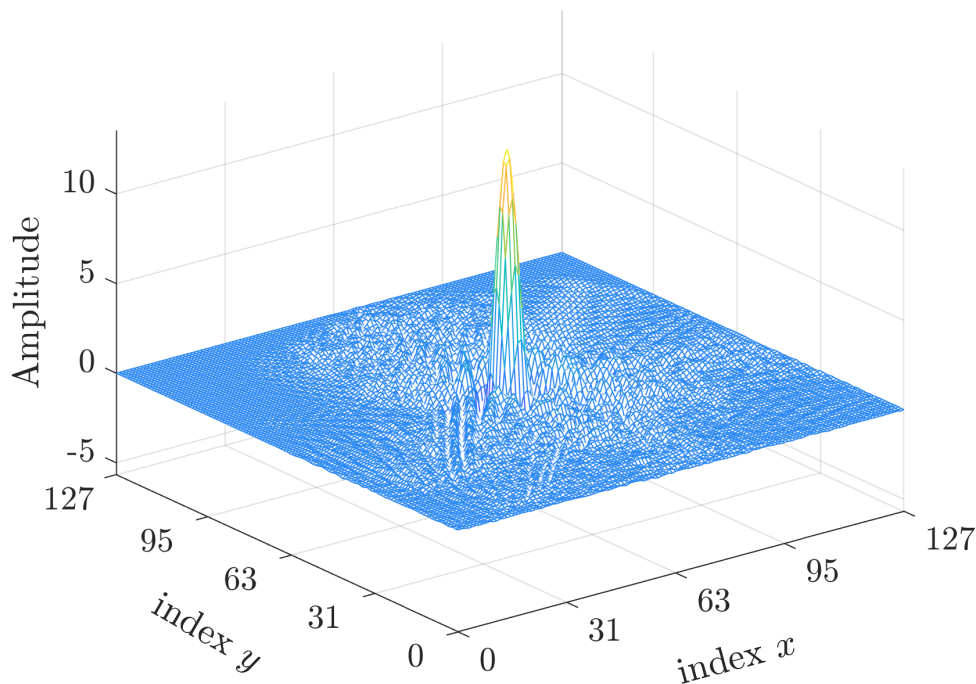


FIGURE 4. The 3D plot of moment distribution of the proposed polynomial in the DKTKCT domain

4. Performance Evaluation of The Proposed Polynomials. This section evaluates the transforms (DCKTT, DCKTKT, and DKTKCT) by providing experimental results. In this section, the computational aspects of the proposed hybrid forms are evaluated in terms of reconstruction of 2D signals, measuring of the localization property, and measuring of the energy compaction (EC) property. In addition, a comparative analysis is performed among the proposed polynomials and the existence polynomials STKP [19], SKTP [17], DKT [11], DTKT [28] to show the robustness of the proposed work.

4.1. The Localization Property. In this subsection, the localization in space property is tested for the proposed polynomials. As mentioned previously, this property determines what frequencies are present and in which part of the signal based on a specific parameter termed as the localization parameter. It determines the ability of the OPs to extract local features and define the quality of all OPs. To examine the property of localization for the proposed polynomials, the procedure described in [31] is employed as follows:

- The matrix of the test image in the moment domain is partitioned into four quarters: q1, q2, q3 and q4.
- To determine the ROI in the test image, a binary mask is used, which has ones in the ROI and zeros in the remaining parts.
- The following equation is used to reconstruct the ROI:

$$\hat{f}(x, y) = \sum_{n=0}^{N-1} \sum_{m=0}^{N-1} R_n(x; N) R_m(y; N) \Phi_{nm}, \quad (44)$$

$$x = 0, 1, \dots, N/2 - 1$$

$$y = 0, 1, \dots, N/2 - 1$$

Figure 5 shows the quarters in the moments domain as well as the reconstructed image quarters. Figure 5b shows the reconstruction of q1 quarter, which reconstructs the region of $f_{x,y=N/2-1}^{N-1}$ using DKTKC transform with 0.183 sec execution time, it can be noted that this type of orthogonal polynomial reverses the signal reconstruction process, while the same reconstruction process occurs for the DCKTK transform as shown in Figure 5c with 0.04 sec execution time. Therefore, DCKTK is better than DKTKC in term of reconstruction quality and execution time. On the other hand, for SKTP to reconstruct the region of $f_{x,y=0}^{N/2-1}$, the second quarter q2 of the image will be reconstructed with 0.385 sec execution time as shown in Figure 5d and when the process is repeated for STKP, Figure 5e shows that the first quarter q1 will be reconstructed with 0.181 sec execution time. Therefore, it can be notice that the DCKTK transform has the best feature extraction property in terms of quality and consumption less processing time, while the DCKTT does not have localization in space.

The results of the variance distribution of the transform coefficient for $N = 8$ and $\rho = 0.8$, and 0.9 are presented in Table 4. It is possible to summarize the variance values of the transform coefficient (σ_l^2) for DTKT, DKTT, STKP, SKTP, and the proposed polynomials with two covariance coefficients $\rho = 0.8$ and $\rho = 0.9$ and $N = 8$ as a function of d , where d denotes the diagonal coefficients. It can infer that the maximum values of variance for DKTT, SKTT, and DKTKC, are located at $D = 4$ and $D = 5$ with the variance gradually decreasing towards the edges, whereas the maximum values of DTKT, STKT, and DCKTK are at the edges and decreases toward the centre. To examine the EC of the proposed transforms, the normalized restriction error (J_m) in [12] is computed as follows:

$$J_m = \frac{\sum_{q=n}^{N-1} \sigma_q^2}{\sum_{q=0}^{N-1} \sigma_q^2}, \quad (45)$$

$$n = 0, 1, \dots, N - 1$$

Where σ_q^2 represents σ_d^2 arranged in descending order. Figure6 illustrates a comparison between the proposed polynomials, while Figure7 illustrates a comparison between DTKT, DKTT, STKP, SKTP and the proposed polynomials, in term of the normalized restriction error with two covariance coefficients values of 0.85 and 0.75.

5. Experimental Results on Different applications.

5.1. Numerical Recognition Application.

As technology and automation continue to evolve, the need for applications such as numerical recognition application increases due to their importance and their entry in diverse fields, including finance, logistics, document digitization and manufacturing, where accuracy and speed of the running time are

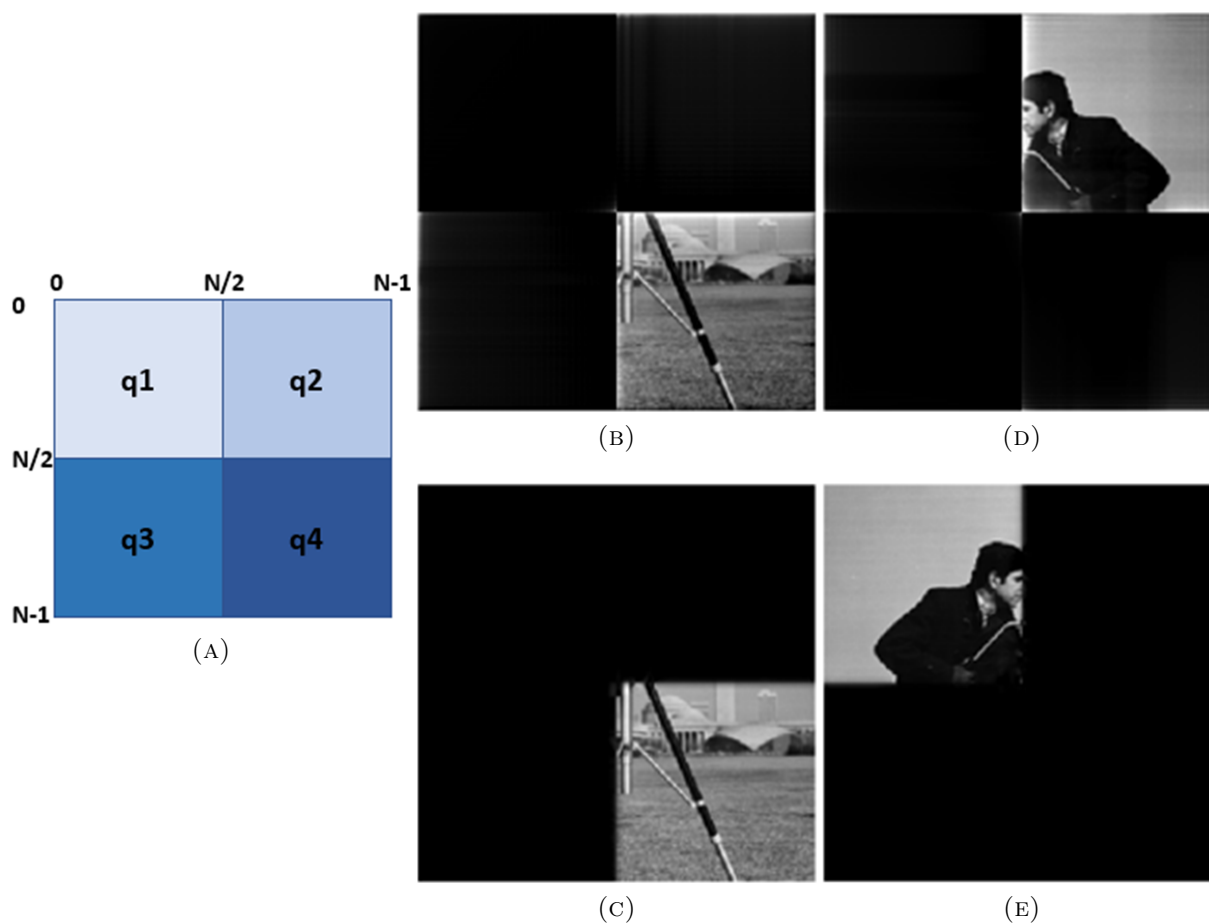
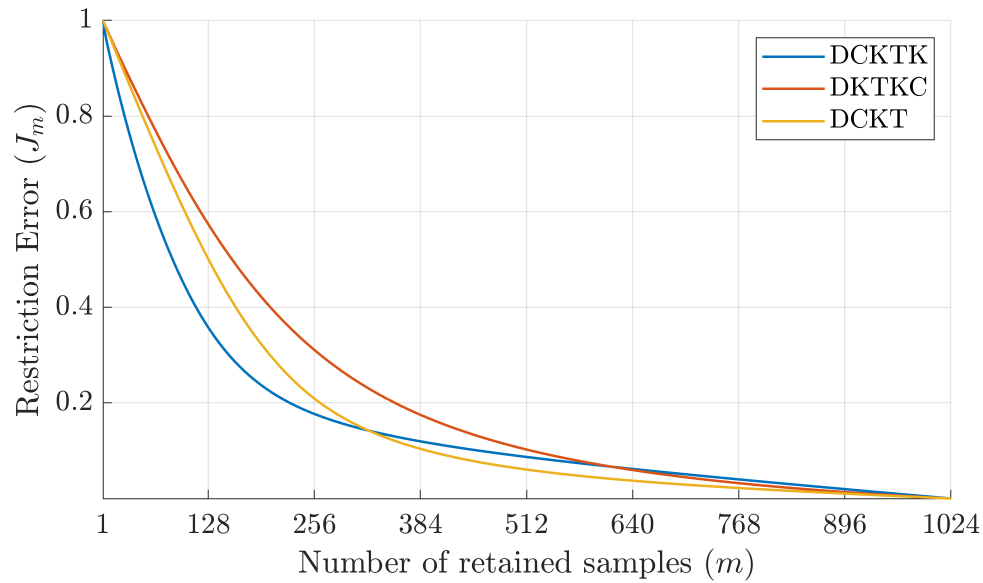


FIGURE 5. (a) Moments domain matrix, (b) Image reconstructed quarter using DKRTKCT, (c) Image reconstructed quarter using DCKTKT, (d) Image reconstructed quarter using SKTP, (e) Image reconstructed quarter using STKP.

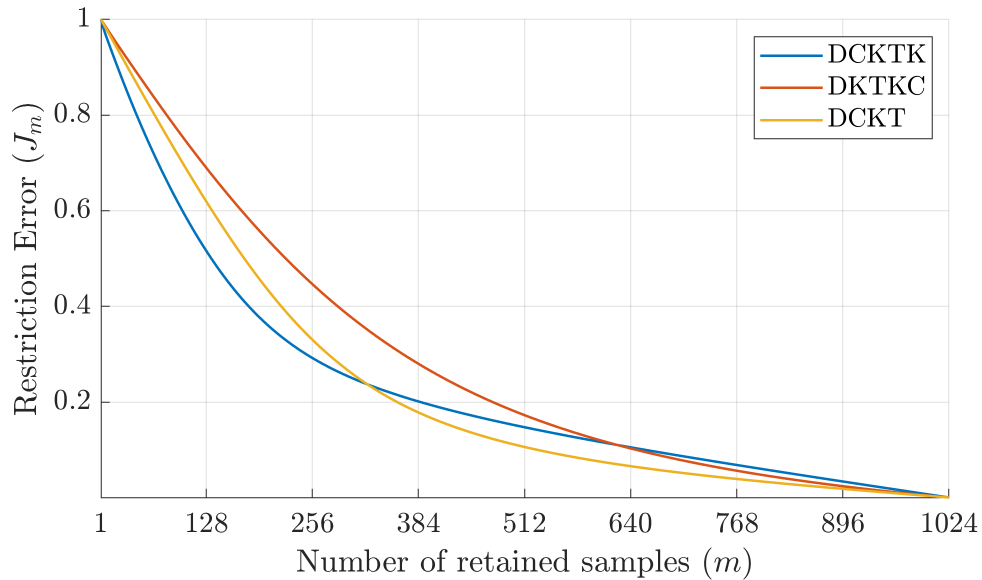
very important factors. Various methodologies are applied to implement the numerical recognition starting from classical support vector machine (SVM) classifiers [50] to advanced convolutional neural networks (CNNs) [51]. In [49] orthogonal polynomials have been implemented by using SKTP polynomial which plays a vital role in enhancing the accuracy and execution time of numerical recognition applications specially in noisy environment, and it shows its robustness against noise distortion and outperforms to all previous methods remarkably.

To clarify the performance of the proposed polynomials in terms of accuracy and execution time, two different environments are used in the experiments: a clean (noise-free) environment and noisy environment. The comparison is performed with SKTP polynomial based on numerical recognition application as a case study.

The flow charts of the implemented numerical recognition process are shown in Figure 8 and Figure 9 which is adopted from the work introduced in [49]. In the recognition process, the first step is based on extracting the features that are used for signal representation in transform domain. The proposed polynomials are adopted then select a specific moments' order and perform a matrix multiplication based on MNIST database images (Training and Testing dataset) to transfer them to moment domain for efficient global features extraction as shown in Figure 8. After that, an identified number value (ID) for each



(A)

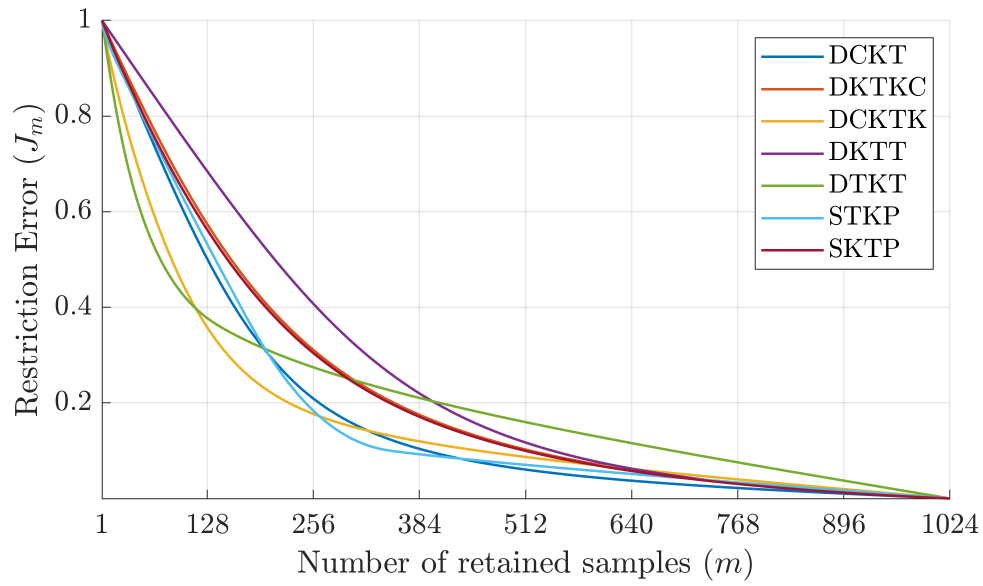


(B)

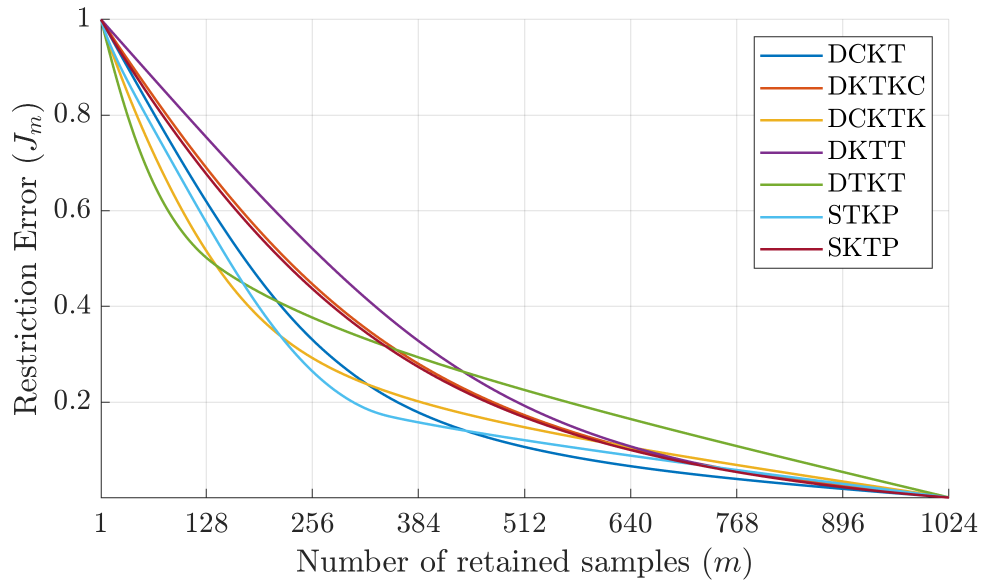
FIGURE 6. Restriction error for the proposed transforms with (a) $\rho = 0.85$, (b) $\rho = 0.75$.

input image is obtained based on a classifier where the SVM method is used in the classification process which is considered as a second step in the recognition process as shown in Figure 9. Then, an evaluation process is performed to check the efficiency of the process by checking the accuracy between the actual and predicted labels.

To evaluate the performance of the proposed polynomials in numerical recognition application, the accuracy comparison is presented between the proposed polynomials and SKTP. The comparisons are conducted for clean and noisy environments using different datasets (Roman and Devanagari) numeral recognition with 10,000 samples for each dataset, which was divided into 5000 for training and 5000 for testing. Details of the datasets used are depicted in Table 1.



(A)



(B)

FIGURE 7. Restriction error for DTKT, DKTT, STKT, SKTT and the proposed polynomials (a) $\rho = 0.85$, (b) $\rho = 0.75$.

TABLE 1. Details of the datasets used in numerical recognition application.

Attribute	Devanagari	Roman
Dataset Name	CMATERdb3.2.1	MNIST
Dataset Reference	[53]	[54]
Script/Numeral System	Devanagari (0-9)	Roman (0-9)
Dataset Name	CMATERdb3.2.1	MNIST
Numerical Numbers	10 (0-9 in Devanagari)	10 (0-9 in Roman)
Samples per Number	300	1000
Total Samples	3000	10000

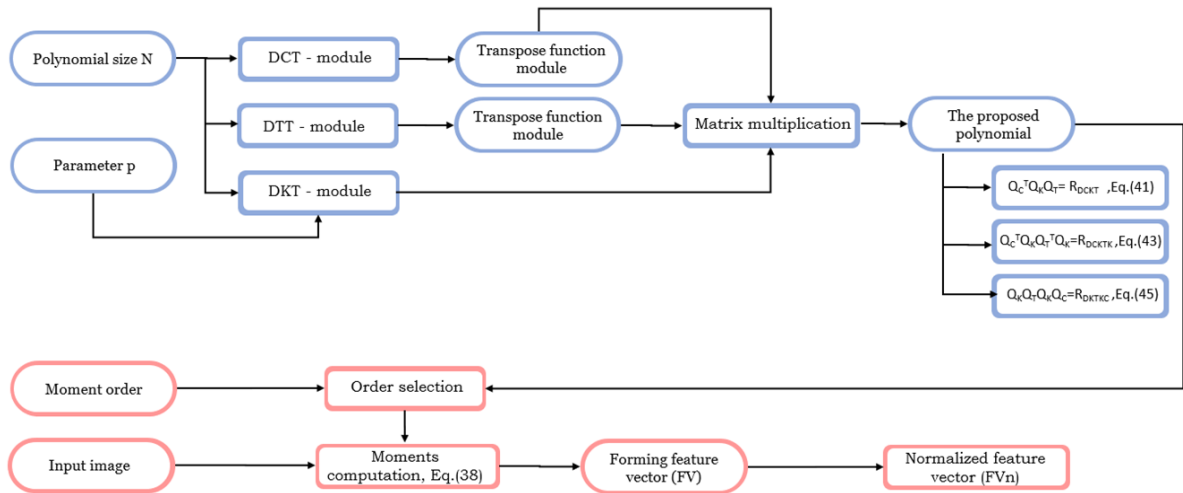


FIGURE 8. Flow diagram of the features extraction process.

Table 2 shows the accuracy evaluation of the proposed functions compared to SKTP in the clean environment where no noise is added. It can be seen that DCKT polynomial presents a higher accuracy as compared to SKTP in noise-free environment, while the DKTKC polynomial gives results close to SKTP, with less complexity in execution time. Therefore, each proposed polynomial has its significant property that gave it the superior property.

In the noisy environment, and as shown in Table 3, the DCKT polynomial also shows higher accuracy with different types of noise that are presented in the table. In general, the proposed transform, DCKT, outperformed other transforms in terms of accuracy and execution time in all types of environments.

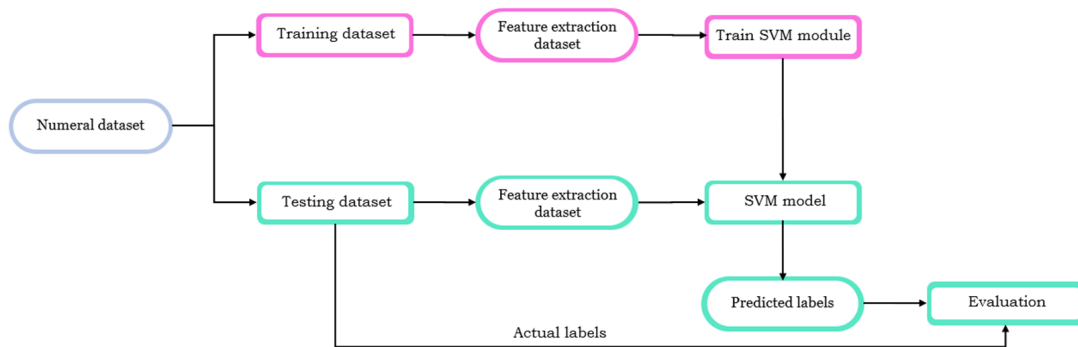


FIGURE 9. Flow diagram of support vector machine (SVM) training and testing process.

5.2. Energy Compaction (EC). EC measures how efficiently a large fraction of the signal energy is captured and represented by a reduced set of transform coefficients [12]. In other words, this property is defined as the ratio of the number of coefficients that include most energy of the signal to the total number of coefficients. When the ratio value is low for a given compression percentage; this means better energy compaction is delivered. The reconstruction of signal information depends on a specific sequence of moment indices that concentrates most of the signal’s energy, while negligible energy appears in the remaining moments. This concentration does not lead to information loss, making the transform

TABLE 2. Comparison between the proposed polynomials and SKTP polynomial for MNIST dataset in clean environment.

Method	Classifier Type	Dataset	Accuracy %	Execution Time
SKTP	SVM	MNIST	99.90	14.18
DCKT	SVM	MNIST	99.96	14.33
DCKTK	SVM	MNIST	99.68	14.27
DKTKC	SVM	MNIST	99.82	13.92

TABLE 3. Comparison between the proposed polynomials and SKTP polynomial for Roman numeral recognition in noisy environment.

	SKTP		DCKT		DCKTK		DKTKC	
	Accuracy %	Execution Time						
Speckle $\sigma^2 = 0.05$	99.84	17.136	99.94	14.422	99.70	17.821	99.88	16.81
Speckle $\sigma^2 = 0.01$	99.86	18.387	99.96	14.382	99.68	17.878	99.82	16.271
poisson	99.86	18.743	99.96	16.462	96.64	20.194	99.86	21.631
Salt & Pepper d = 0.05	99.44	17.271	97.86	14.375	96.84	18.006	98.70	28.532
Salt & Pepper d = 0.01	99.82	16.559	99.94	16.502	99.64	17.846	99.82	16.316

suitable for compression applications. Therefore, a comparison is performed first between the three proposed polynomials, second between DTKT, DKTT, STKP, and SKTP hybrid form and the proposed polynomials, using the procedure presented by [12], which is based on stationary Markov sequence of the first-order with zero mean and length N as follows:

1. A covariance matrix M with different covariance coefficient ρ , is given by [12]:

$$\mathcal{M} = \begin{bmatrix} 1 & \rho & \rho^2 & \cdots & \rho^{N-1} \\ \rho & 1 & \cdots & \cdots & \vdots \\ \rho^2 & \vdots & \ddots & \vdots & \rho^2 \\ \vdots & \cdots & \cdots & \ddots & \rho \\ \rho^{N-1} & \cdots & \rho^2 & \rho & 1 \end{bmatrix}. \quad (46)$$

2. Multiply the M matrix by the proposed polynomial to transform it to the moment domain using the following equation:

$$T = R M R^T \quad (47)$$

where R is the matrix form of the OP, and T is the transformed matrix that is used to describe the transform coefficients that are denoted by the diagonal T .

5.3. Digital Image Steganography Application. The rapid evolution of digital technologies has significantly increased the volume and importance of sensitive data being transmitted and stored. Due to growing concerns over unauthorized access, data breaches,

TABLE 4. The distribution of variance of the transform coefficient for $N = 8$ and $\rho = 0.8$, and 0.9 .

D	$\rho=0.8$							$\rho=0.9$						
	DTKT	DKTT	STKT	SKTT	DCKT	DCKTK	DKTKC	DTKT	DKTT	STKT	SKTT	DCKT	DCKTK	DKTKC
1	2.336	0.254	3.031	0.188	3.862	3.083	0.226	2.585	0.16	3.402	0.108	4.956	3.487	0.129
2	0.659	0.676	0.457	0.349	1.834	0.425	0.399	0.571	0.568	0.257	0.187	1.606	0.248	0.219
3	0.526	1.295	0.269	1.016	1.118	0.267	1.002	0.446	1.309	0.183	0.869	0.846	0.137	0.863
4	0.479	1.774	0.242	2.446	0.500	0.225	2.373	0.398	1.964	0.158	2.836	0.262	0.129	2.79
5	0.479	1.774	0.242	2.446	0.263	0.225	2.373	0.398	1.964	0.158	2.836	0.129	0.129	2.79
6	0.526	1.295	0.269	1.016	0.173	0.267	1.002	0.446	1.309	0.183	0.869	0.083	0.137	0.863
7	0.659	0.676	0.457	0.349	0.133	0.425	0.399	0.571	0.568	0.257	0.187	0.064	0.248	0.219
8	2.336	0.254	3.031	0.188	0.118	3.083	0.226	2.585	0.16	3.402	0.108	0.056	3.487	0.129

TABLE 5. Comparison between the proposed polynomials and SKTP polynomial for Devanagari numeral recognition in noisy environment.

	SKTP		DCKT		DCKTK		DKTKC	
	Accuracy %	Execution Time						
Speckle $\sigma^2 = 0.05$	98.87	42.18	99.43	56.41	99.37	55.69	98.83	43.41
Speckle $\sigma^2 = 0.01$	98.87	43.37	99.40	58.76	99.33	55.26	98.90	44.38
poisson	98.90	41.40	99.40	58.98	99.37	54.25	98.90	45.99
Salt & Pepper $d = 0.05$	98.87	39.41	99.43	55.75	99.27	55.33	98.3	52.06
Salt & Pepper $d = 0.01$	98.93	42.84	99.40	58.58	99.37	52.62	98.93	45.90

and privacy violations, the development and implementation of advanced information hiding techniques have become critical to ensuring the security and integrity of data [55].

To further explain the performance ability, this section presents a second case study to evaluate the efficacy of the proposed OP, where the digital image steganography application is implemented. The flow chart of implementation steganography process is shown in Figure 10 which is similar to steganography workflow introduced in [56]. In that work, SKTP shows a high EC, and localization properties when compared to other hybrid forms [56]. In this case, the presented hybrid OPs are compared to SKTP in the steganography process to evaluate their performance.

The first step in steganography process is to convert the image from spatial domain to moments domain using DCKT, DCKTK, and DKTKC (Eqs. (39), (41), and (43)). Secondly, the moments are obtained with the high energy using a binary mask to preserve the image information, as shown in Figure11. Each transform has its own moment distribution and the mask values are set to ones in the ROI (required part) and zeros in the remaining parts. Then, the values of the secret image are normalized to be equal

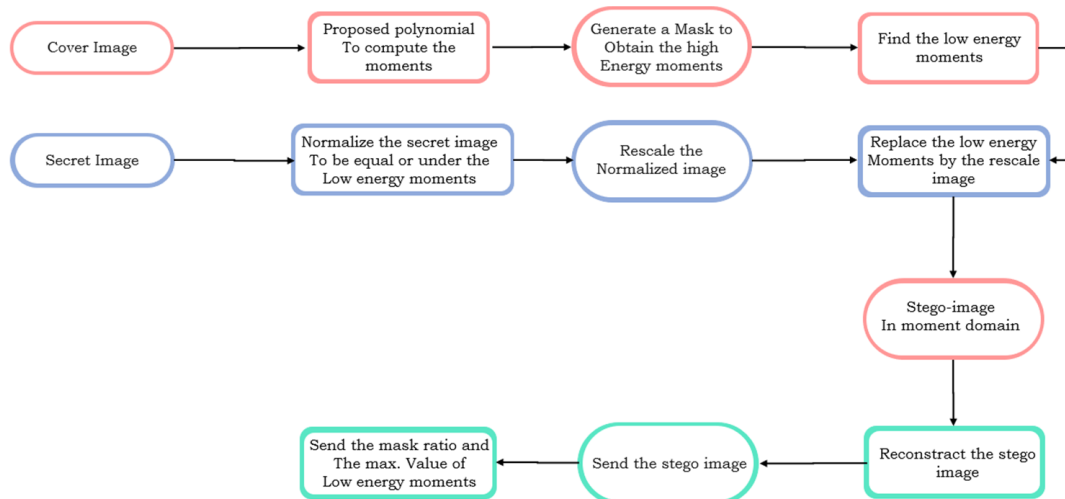


FIGURE 10. The flow diagram of the Steganography application using different types of OP.

TABLE 6. PSNR comparison results of the polynomials and SKTP using a cover image of size (a) 128×128 , and (b) 64×64

(A) 128×128

Cover image	SKTP	DCKT	DCKTK	DKTKC
Birds	50.219	55.087	49.484	52.725
Boat	49.219	55.319	44.880	49.902
Couple	49.505	50.629	45.078	48.694
F-16	53.149	58.319	45.605	54.353
Hill	48.627	54.204	45.001	50.712
House	47.441	55.659	47.115	47.071
Average	49.693	54.870	46.194	50.576

(B) 64×64

Cover image	SKTP	DCKT	DCKTK	DKTKC
Birds	57.632	60.207	58.920	62.656
Boat	58.152	64.181	52.650	61.816
Couple	57.162	57.619	50.942	56.484
F-16	62.605	66.049	51.371	64.604
Hill	56.099	61.605	51.162	61.122
House	57.188	63.174	55.130	57.479
Average	58.140	62.139	53.363	60.694

or under the low energy moments and resized to be placed where the mask values equal to zero. The stego-image is reconstructed to spatial domain and sent with its required information to the receiver.

To appraise the performance of the hybrid forms, two types of measurements have been used: peak signal-to-noise-ratio (PSNR) and SSIM, where the size of the cover images is 512×512 and two different sizes for the secret image have been employed, which are 128×128 and 64×64 .

Table 6 illustrates the comparison results between SKTP [56] and the proposed hybrid forms in terms of PSNR. It can be noted that the PSNR values for DCKT and DKTKCT are acceptable compared to SKTP across different message sizes. For example, the average PSNR for secret image size 128×128 is 54.850 and 50.576 for DCKT and DKTKCT, respectively, while the average PSNR for secret image size 64×64 is 62.140 and 60.694 for DCKT and DKTKCT, respectively.

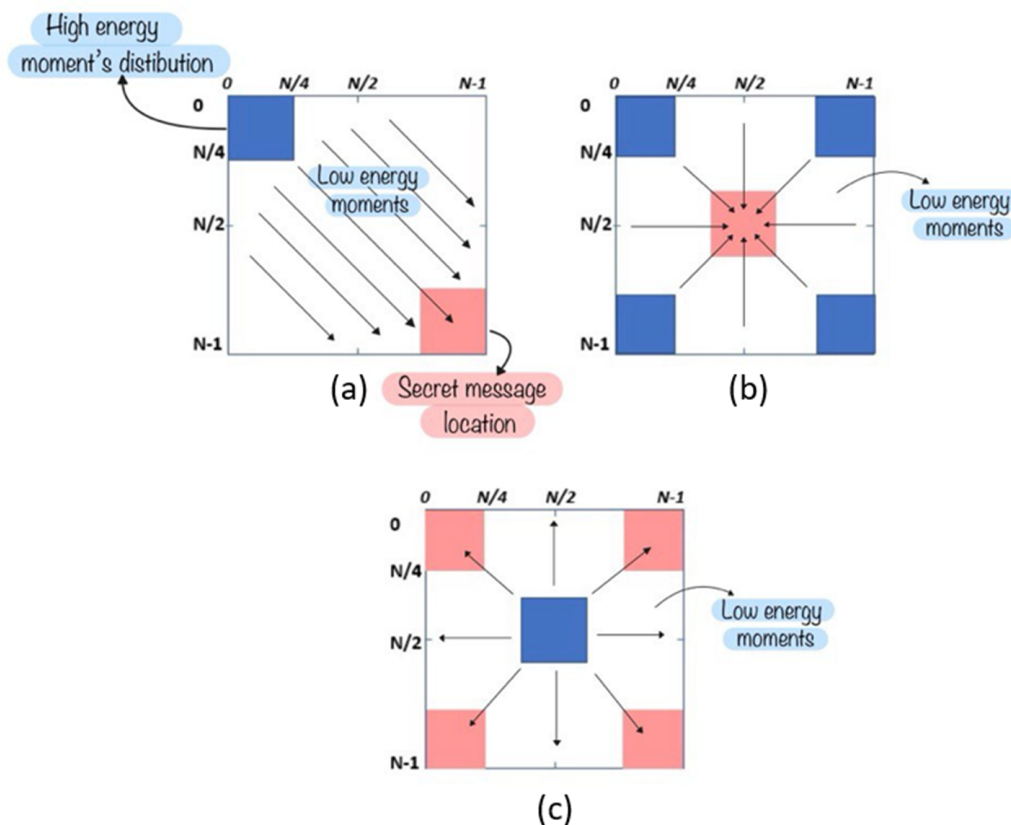


FIGURE 11. High energy moments distribution for the proposed polynomials, and locations of secret messages, (a)DCKT, (b) DCKTK, (c) DKTKC

For more evaluation, Figure 12 shows the quality of the stego-images generated using DCKTK polynomial for secret image sizes of 64×64 and 128×128 . The cover image are shown in the first column, while the middle and the last columns show the stego-image embedded with secret image of size 64×64 and 128×128 , respectively. It is evident that there are no noticeable distortion by the human eye between the cover-image and the stego-images.

6. Conclusion. In this paper, a new set of discrete orthogonal functions were proposed. The proposed OPs are constructed by multiplying well-known OPs. DCT is employed as a substantial part of the proposed hybrid forms of OP and their moments computations. The proposed hybrid forms are termed as: DCKT, DKTKC, and DCKTK and derived from three transforms which are DCT, DKrT and DThT. The proposed DCKT shows superior performance in terms of EC as compared with DKTKC, DCKTK and other existing hybrid forms of KrP and TcP; while DKTKC and DCKTK outperform other transforms in terms of localization property and DCKTK has the best features extraction as compared with other hybrid forms. A comparative study is performed using two



FIGURE 12. Cover images with their corresponding stego-images obtained from the DCKTK polynomial.

applications: digital image steganography and numerical recognition applications. DCKT shows a remarkable result as compared with existing OPs in the two applications, while the DCKTK and DKTKC show results that are close to existing OPs, with an improvement in terms of execution time in some results. However, the proposed hybrid forms have the potential to show better and improved results in different computer vision applications such as compression applications, indicating a possible direction for future work.

Acknowledgment. The authors would like to thank University of Baghdad for their general support. The authors also gratefully acknowledge the helpful comments and suggestions of the reviewers, which have improved the presentation.

REFERENCES

- [1] S. Roy and A. Chandra, "A Survey of FIR Filter Design Techniques: Low-complexity, Narrow Transition-band and Variable Bandwidth," *Integration*, vol. 77, no. 8, pp. 193–204, 2021. [Online]. Available: <https://doi.org/10.1016/j.vlsi.2020.12.001>
- [2] B. Torres, G. Peeters, and G. Richard, "Unsupervised Harmonic Parameter Estimation Using Differentiable DSP and Spectral Optimal Transport," pp. 1–5, 2023. [Online]. Available: <http://arxiv.org/abs/2312.14507>
- [3] R. B. Pachori, *Time-Frequency Analysis Techniques and their Applications*, 2023.
- [4] W. Liu, E. W. Hu, B. Su, and J. Wang, "Using machine learning techniques for DSP software performance prediction at source code level," *Connection Science*, vol. 33, no. 1, pp. 26–41, 2021. [Online]. Available: <https://doi.org/10.1080/09540091.2020.1762542>
- [5] S. H. Abdulhussain, A. R. Ramli, S. A. R. Al-Haddad, B. M. Mahmmod, and W. A. Jassim, "On Computational Aspects of Tchebichef Polynomials for Higher Polynomial Order," *IEEE Access*, vol. 5, no. c, pp. 2470–2478, 2017.
- [6] B. M. Mahmmod, A. M. Abdul-Hadi, S. H. Abdulhussain, and A. Hussien, "On computational aspects of krawtchouk polynomials for high orders," *Journal of Imaging*, vol. 6, no. 8, 2020.
- [7] S. H. Abdulhussain, A. R. Ramli, S. A. R. Al-Haddad, B. M. Mahmmod, and W. A. Jassim, "Fast Recursive Computation of Krawtchouk Polynomials," *Journal of Mathematical Imaging and Vision*, vol. 60, no. 3, pp. 285–303, 2018.
- [8] X.-M. Huang, Y. Lin, and Y.-Q. Zhao, "Asymptotics of the charlier polynomials via difference equation methods," *Analysis and Applications*, vol. 19, no. 04, pp. 679–713, 2021.
- [9] Z. I. Abood, "Image Compression Using 3-D Two-Level Techniques," vol. 19, no. 11, 2013.
- [10] L. Kotoulas and I. Andreadis, "Image moments based on hahn polynomials," *IEEE Transactions on Pattern Analysis and Machine Intelligence*, vol. 29, pp. 2057–2062.
- [11] B. M. Mahmmod, A. R. bin Ramli, S. H. Abdulhussain, S. A. R. Al-Haddad, and W. A. Jassim, "Signal compression and enhancement using a new orthogonal-polynomial-based discrete transform," *IET Signal Processing*, vol. 12, no. 1, pp. 129–142, feb 2018.
- [12] A. K. Jain, "Fundamentals of Digital Image Processing," Tech. Rep.
- [13] H. Zenkouar and A. Nachit, "Images compression using moments method of orthogonal polynomials," *Materials Science and Engineering: B*, vol. 49, no. 3, pp. 211–215, 1997.
- [14] "Improved image compression based wavelet transform and threshold entropy," *Journal of Engineering*, vol. 17, no. 05, p. 1152–1158, Oct. 2011. [Online]. Available: <https://www.joe.uobaghdad.edu.iq/index.php/main/article/view/3003>
- [15] N. Y. Balthoon, "Combined dwt and dct image compression using sliding rle technique," *Baghdad Science Journal*, vol. 8, no. 3, pp. 238–238, 2011.
- [16] A. H. Ahmed and L. E. George, "The use of wavelet, dct & quadtree for images color compression," *Iraqi Journal of Science*, pp. 550–561, 2017.
- [17] S. H. Abdulhussain, A. R. Ramli, B. M. Mahmmod, M. I. Saripan, S. A. Al-Haddad, and W. A. Jassim, "A New Hybrid form of Krawtchouk and Tchebichef Polynomials: Design and Application," *Journal of Mathematical Imaging and Vision*, vol. 61, no. 4, pp. 555–570, may 2019.
- [18] Y. El Madmoune, I. El Ouariachi, K. Zenkouar, and A. Zahi, "Robust face recognition using convolutional neural networks combined with krawtchouk moments." *International Journal of Electrical & Computer Engineering (2088-8708)*, vol. 13, no. 4, 2023.
- [19] Z. N. Idan, S. H. Abdulhussain, and S. A. R. Al-Haddad, "A New Separable Moments Based on Tchebichef-Krawtchouk Polynomials," *IEEE Access*, vol. 8, pp. 41 013–41 025, 2020.
- [20] A. L. N. Abbas, "Implementations of 8x8 dct and idct on different fpga technologies using the modified loeffler algorithm," 2005.
- [21] L. E. George, F. G. Mohammed, and I. A. Taqi, "Effective image watermarking method based on dct," *Iraqi Journal of Science*, vol. 56, no. 3B, pp. 2374–2379, 2015.
- [22] A. M. Salih and S. H. Mahmood, "Digital color image watermarking using encoded frequent mark," *Journal of Engineering*, vol. 25, no. 3, pp. 81–88, 2019.

- [23] K. K. Jabbar, F. Ghozzi, and A. Fakhfakh, "Robust color image encryption scheme based on rsa via dct by using an advanced logic design approach," *Baghdad Science Journal*, vol. 20, no. 6 (Suppl.), pp. 2593–2593, 2023.
- [24] L. Tan, Q. Wang, H. Zheng, and Y. Si, "Subpixel edge contour extraction based on zernike orthogonal moments," in *Proceedings of the 7th International Conference on Intelligent Information Processing*, 2022, pp. 1–6.
- [25] S. J. Abou-Loukh, T. Zeyad, and R. Thabit, "Ecg classification using slantlet transform and artificial neural network," *Journal of Engineering*, vol. 16, no. 01, pp. 4510–4526, 2010.
- [26] A. S. A. AL-Jumaili, H. K. Tayyeh, and A. Alsadoon, "Alexnet convolutional neural network architecture with cosine and hamming similarity/distance measures for fingerprint biometric matching," *Baghdad Science Journal*, vol. 20, no. 6 (Suppl.), pp. 2559–2559, 2023.
- [27] M. A. Rajab and L. E. George, "Car logo image extraction and recognition using k-medoids, daubechies wavelets, and dct transforms," *Iraqi Journal of Science*, pp. 431–442, 2024.
- [28] W. A. Jassim and P. Raveendran, "Face recognition using Discrete Tchebichef-Krawtchouk Transform," *Proceedings - 2012 IEEE International Symposium on Multimedia, ISM 2012*, no. December 2012, pp. 120–127, 2012.
- [29] W. A. Jassim, "A New Discrete Orthogonal Function Based on Tchebichef and Krawtchouk Polynomials and Its Applications to Speech and Image Analysis," Ph.D. dissertation, Universiti Malaya, 2012.
- [30] R. Mukundan, S. H. Ong, and P. A. Lee, "Image analysis by Tchebichef moments," *IEEE Transactions on Image Processing*, vol. 10, no. 9, pp. 1357–1364, 2001.
- [31] R. Mukundan, "Some computational aspects of discrete orthonormal moments," *IEEE Transactions on Image Processing*, vol. 13, no. 8, pp. 1055–1059, 2004.
- [32] P. T. Yap, R. Paramesran, and S. H. Ong, "Image analysis by Krawtchouk moments," *IEEE Transactions on Image Processing*, vol. 12, no. 11, pp. 1367–1377, 2003.
- [33] K. Manasa and V. Krishnaveni, "Certain investigation on brain tumour segmentation using discrete orthogonal moments approach on u-net," *Neuroquantology*, vol. 20, no. 7, p. 3837, 2022.
- [34] M. Asakura and T. Yabu, "Explicit logarithmic formulas of special values of hypergeometric functions ${}_3F_2$," *Communications in Contemporary Mathematics*, vol. 22, no. 05, p. 1950040, 2020.
- [35] S. R. KABARA, "New generalized hypergeometric functions," *Ikonion Journal of Mathematics*, vol. 4, no. 2, pp. 21–31, 2022.
- [36] W. Gautschi, "Computational aspects of three-term recurrence relations," *SIAM review*, vol. 9, no. 1, pp. 24–82, 1967.
- [37] —, "Minimal solutions of three-term recurrence relations and orthogonal polynomials," *mathematics of computation*, vol. 36, no. 154, pp. 547–554, 1981.
- [38] M. Begum, J. Ferdush, and M. S. Uddin, "A Hybrid robust watermarking system based on discrete cosine transform, discrete wavelet transform, and singular value decomposition," *Journal of King Saud University - Computer and Information Sciences*, vol. 34, no. 8, pp. 5856–5867, 2022. [Online]. Available: <https://doi.org/10.1016/j.jksuci.2021.07.012>
- [39] B. S. Journal, "Orthogonal Functions Solving Linear functional Differential Equations Using Chebyshev Polynomial," *Baghdad Science Journal*, vol. 5, no. 1, pp. 143–148, 2008.
- [40] A. Setyono and D. R. Ignatius Moses Setiadi, "An image watermarking method using discrete tchebichef transform and singular value decomposition based on chaos embedding." *International Journal of Intelligent Engineering & Systems*, vol. 13, no. 2, 2020.
- [41] B. Honarvar Shakibaei Asli and M. H. Rezaei, "Four-term recurrence for fast krawtchouk moments using clenshaw algorithm," *Electronics*, vol. 12, no. 8, p. 1834, 2023.
- [42] A. Bagdasaryan, "A note on the $2F_1$ hypergeometric function," *arXiv preprint arXiv:0912.0917*, 2009.
- [43] H. Zhu, M. Liu, H. Shu, H. Zhang, and L. Luo, "General form for obtaining discrete orthogonal moments," *IET Image Processing*, vol. 4, no. 5, pp. 335–352, 2010.
- [44] G. Zhang, Z. Luo, B. Fu, B. Li, J. Liao, X. Fan, and Z. Xi, "A symmetry and bi-recursive algorithm of accurately computing krawtchouk moments," *Pattern Recognition Letters*, vol. 31, no. 7, pp. 548–554, 2010.
- [45] N. Ahmed, T. Natarajan, and K. R. Rao, "Discrete cosine transform," *Computers, IEEE Transactions on*, vol. C-23, no. 1, pp. 90–93, 1974.
- [46] A. K. Shakya and A. Vidyarthi, "Comprehensive study of compression and texture integration for digital imaging and communications in medicine data analysis," *Technologies*, vol. 12, no. 2, p. 17, 2024.

- [47] V. Dave, H. Borade, H. Agrawal, A. Purohit, N. Padia, and V. Vakharia, "Deep learning-enhanced small-sample bearing fault analysis using q-transform and hog image features in a gru-xai framework," *Machines*, vol. 12, no. 6, p. 373, 2024.
- [48] X. Liu and W. Wang, "Deep time series forecasting models: A comprehensive survey," *Mathematics*, vol. 12, no. 10, p. 1504, 2024.
- [49] S. H. Abdhussain, B. M. Mahmmod, M. A. Naser, M. Q. Alsabab, R. Ali, and S. A. Al-Haddad, "A robust handwritten numeral recognition using hybrid orthogonal polynomials and moments," *Sensors*, vol. 21, no. 6, pp. 1–18, 2021.
- [50] D. Gorgevik and D. Cakmakov, "Handwritten digit recognition by combining SVM classifiers," in *EUROCON 2005-The International Conference on "Computer as a Tool"*, vol. 2. IEEE, 2005, pp. 1393–1396.
- [51] R. Jana, S. Bhattacharyya, and S. Das, "Handwritten digit recognition using convolutional neural networks," *Deep Learning: Research and Applications*, pp. 51–68, 2020.
- [52] W. A. Jassim, P. Raveendran, and R. Mukundan, "New orthogonal polynomials for speech signal and image processing," *IET Signal Processing*, vol. 6, no. 8, pp. 713–723, 2012.
- [53] "Cmaterdb." [Online]. Available: <https://code.google.com/archive/p/cmaterdb/downloads>
- [54] Y. LeCun, C. Cortes, C. Burges *et al.*, "Mnist handwritten digit database," 2010.
- [55] T.-K. Dao, T.-T. Nguyen, T.-X.-H. Nguyen, and T.-D. Nguyen, "Recent information hiding techniques in digital systems: A review." *Journal of Information Hiding and Multimedia Signal Processing*, vol. 15, no. 1, pp. 10–20, 2024.
- [56] H. S. Radeaf, B. M. Mahmmod, S. H. Abdhussain, and D. Al-Jumaeily, "A steganography based on orthogonal moments," in *Proceedings of the international conference on information and communication technology*, 2019, pp. 147–153.